

FakeLocator: Robust Localization of GAN-Based Face Manipulations

Yihao Huang
East China Normal University
China

Felix Juefei-Xu
Alibaba Group
USA

Run Wang
Nanyang Technological University
Singapore

Qing Guo
Nanyang Technological University
Singapore

Xiaofei Xie
Nanyang Technological University
Singapore

Lei Ma
Kyushu University
Japan

Jianwen Li
East China Normal University
China

Weikai Miao
East China Normal University
China

Yang Liu
Nanyang Technological University
Singapore

Geguang Pu
East China Normal University
China

ABSTRACT

Nowadays, full face synthesis and partial face manipulation by virtue of the generative adversarial networks (GANs) have raised wide public concerns. In the multi-media forensics area, detecting and ultimately locating the image forgery have become imperative. We investigated the architecture of existing GAN-based face manipulation methods and observed that the imperfection of upsampling methods therewithin could be served as an important asset for GAN-synthesized fake images detection and forgery localization. Based on this basic observation, we have proposed a novel approach to obtain high localization accuracy, at full resolution, on manipulated facial images. To the best of our knowledge, this is the very first attempt to solve the GAN-based fake localization problem with a gray-scale fakeness prediction map that preserves more information of fake regions. To improve the universality of *FakeLocator* across multifarious facial attributes, we introduce an attention mechanism to guide the training of the model. Experimental results on the CelebA and FFHQ databases with seven different state-of-the-art GAN-based face generation methods show the effectiveness of our method. Compared with the baseline, our method performs two times better on various metrics. Moreover, the proposed method is robust against various real-world facial image degradations such as JPEG compression, low-resolution, noise, and blur.

KEYWORDS

DeepFake, Face Manipulation, Localization

1 INTRODUCTION

Every day we receive newsletters from the media channels such as television, social media, newspaper, *etc.* Limited by the presentation of these media, compared with text descriptions, the information with images and videos is prone to be accepted by humans and thus becomes more trustworthy to us. However, with the development of digital manipulation technologies, even videos can be synthesized

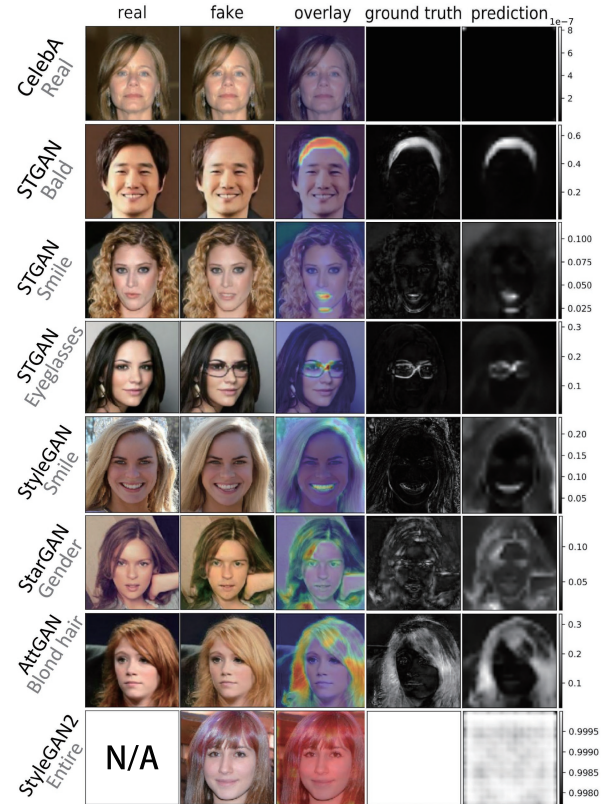


Figure 1: Fake region localization results. These are the results of different GANs and properties. In the left comments, CelebA [20] is a real image database and others are GAN-based face generation methods. The gray text represent facial property. Fake image is produced by manipulating corresponding real image through GAN-based face generation method. Ground truth is calculated by fake image and real image. Fake image and ground truth are the input and output of our method. Overlay is combined of prediction and fake image. The prediction has colorbar which shows the value range of pixels. For the first row which uses real image of CelebA as input, for unity of the figure, we also regard it as fake image.

at a small price. In recent years, a lot of synthetic videos represented by celebrities [27] existed. They were produced by a series of techniques that can produce fake images, audios, and videos, collectively called DeepFake [5]. DeepFake has been widely used in politics and pornography [16, 31]. Fake images can be created easily for that many free tools are available to us. Public concerns about fraud and credibility problems have been raised by such misinformation. Hence, it is urgent to study effective and robust methods in face forgery detection and forensics, for both reality and justice.

The facial images synthesized by GAN-based methods are more authentic than other methods. Due to the potential security and privacy issues of synthesized facial images, researchers have a great interest in detecting images generated by GAN-based methods. Recently, many studies have worked on classifying images with various methods [4, 21, 33, 35]. However, none of them considers locating fake regions of fake images while modifications of facial properties are really common. Localization is more significant and valuable in the research field of multi-media forensics.

In multi-media forensics of facial image, a good localization method would better satisfy the following requirements. (1) The localization map is a high resolution with fine-grained fake regions represented (high-resolution). Because it is important to get a good visualization in real forensics scenarios. (2) The method is robust (robustness), which is important for locators to be deployed in the wild. (3) The method is universal enough to tackle unknown facial properties (universality).

FaceForensics++ [27] is widely used in DeepFake research, but fake videos in **FaceForensics++** exhibit severe artifacts which can be easily detected with existing fake localization methods [17, 22, 28]. Moreover, **FaceForensics++** containing only face identity or expression swap, which is not suitable for demonstrating the effect of fake localization methods. Thus, we build our own dataset with available GANs to generate high-quality forgery images for evaluating the effectiveness and robustness of our proposed method. To the best of our knowledge, only [29] working on the same topic as us. Therefore, we select their method as the only baseline in the experiment of us. In the literature, they insert an attention map module into a classifier such as Xception [3] to obtain the location of fake regions. However, the resolution of the attention map is constrained by their design and can only output a tiny map. For example, an image of size 299x299 obtains an attention map of size 19x19. So the attention map can not exactly pinpoint out the fake regions. All the localization methods mentioned above do not satisfy high-resolution, universality, robustness simultaneously. In addition, the fakeness prediction maps of all these localization methods either for videos or images have several omissions, which will be introduced and improved in our method.

The generators in GAN-based face generation methods are typical encoder-decoder architecture with an upsampling design in its decoder. The upsampling design is used to magnify the feature maps produced by the encoder to be a colorful image. However, the upsampling design may introduce special features into synthesized images. According to the investigation of us, there are only three kinds of upsampling methods. The textures produced by all these upsampling methods contain special features, which are called **fake texture**. We observe that the **fake texture** can not only be used for fake detection, but also used for fake localization. Thus we propose

a universal pipeline that is suitable for the fake localization problem. As an improvement, we also introduce attention mechanism into the architecture to learn **fake texture** better and generalize our approach in unseen facial properties.

The main contributions are summarized as follows.

- We have a new observation that the artifact induced by GAN-based face generation methods could be used in DeepFake forensics including detection and localization. The pipeline proposed by us can locate the manipulated facial regions effectively at full resolution.
- To improve the universality of the model, we introduce the attention mechanism into our framework by using face parsing. The fake textures are captured by the gray-scale fakeness prediction map proposed by us.
- Experiments are conducted on seven state-of-the-art (SOTA) GAN-based face generation methods and two databases. Experimental results show that our approach outperforms prior work [29] in locating fake regions. Furthermore, our method is also robust against various real-world facial image degradations.

2 RELATED WORK

2.1 GAN-based Face Generation

GAN has drawn attention from both academic and industry since first proposed in 2014 [7]. The GAN-based face generation methods can be classified into two categories: full face synthesis and partial face manipulation methods. Here we will introduce seven state-of-the-art GAN-based face generation methods. IcGAN [25], AttGAN [10], StarGAN [2] and STGAN [19] are partial face manipulation methods, PGGAN [12] and StyleGAN2 [14] are full face synthesis methods. StyleGAN [13] is not only a partial face manipulation method, but also a full face synthesis method.

IcGAN [25] introduces the encoder that allows the network to reconstruct and modify real face images with arbitrary attributes. PGGAN [12] proposed progressively growing on both the generator and discriminator to obtain big high-resolution images. StarGAN [2] simply uses a single model to perform image-to-image translations for multiple facial properties. AttGAN [10] applies an attribute classification constraint to the generated image to guarantee the correct change of desired attributes. STGAN [19] simultaneously improves attribute manipulation accuracy as well as perception quality on the basis of AttGAN. StyleGAN [13] proposed a new generator to learn unsupervised separation of high-level attributes and stochastic variation in the generated images. Recently, StyleGAN2 [14] fixed the imperfection of StyleGAN to improve image quality.

These seven SOTA GAN-based methods fully represent GAN-based full face synthesis and partial face manipulation methods. Thus we verify the effectiveness of our method on these seven GAN-based methods. In the following sections, **seven GAN-based face generation methods** is referred to the GANs introduced here, unless particularly addressed.

2.2 Manipulated Face Localization

Only several works have been proposed on the manipulated face localization problem. [28] proposes an architecture to predict face

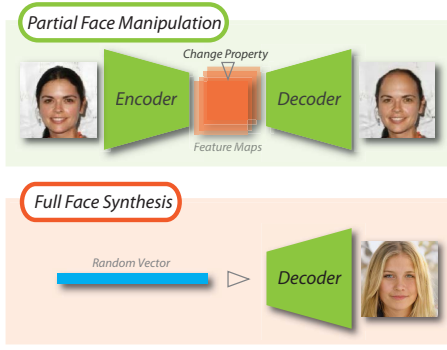


Figure 2: The architecture of GAN-based face generation methods. The top subplot shows how partial face manipulation is carried out. The bottom subplot shows how full face synthesis is carried out.

forensic localization. [22] uses a multi-task learning approach to simultaneously detect manipulated videos and locate the manipulated regions. [17] proposes face X-ray to locate the fake regions. However, the method fails when the image is entirely synthetic. Furthermore, the testing datasets used by them are videos which focus on face swap. The fake regions are very large and easy to locate. We mainly focus on locating modified facial properties. The task of us is much harder than theirs for that the fake regions of facial properties are much smaller.

Only [29] working on the same topic as us. They present the first and only technique that applies the attention mechanism to address the problem. The attention map is advantageous to be added into arbitrary networks and help to improve detection accuracy. However, the attention map is too small to point out the fake regions in the fine-grained level.

To sum up, all the localization methods above do not satisfy high-resolution, universality, robustness simultaneously. Furthermore, the fakeness prediction maps used by these methods are all incomplete, which lose the information about fake regions.

3 IMPERFECTION OF GAN-BASED METHODS

3.1 Architecture

There are mainly two ways to generate facial images: full face synthesis and partial face manipulation. We call these two methods **face generation methods**. Their typical architecture is an encoder-encoder framework shown in Figure 2.

As shown in Figure 2, for all the partial face manipulation methods, the encoder compresses the real image into some small feature maps by convolution and pooling layers. After changing the feature maps with specific facial properties, the modified feature maps are amplified by the upsampling methods in the decoder to be a high-resolution fake image. In full face synthesis, the input is a random vector. Similarly, it also needs to go through a decoder to become an entire fake face image. We can find that all the GAN-based face generation methods have the procedure which amplifies the images from low-resolution to high-resolution. In the magnification process, images are inserted with a lot of new pixels calculated by existing pixels. Hence, the output fake face images of these GAN-based methods inevitably contain fake texture which can not be obtained from the real world through a camera.

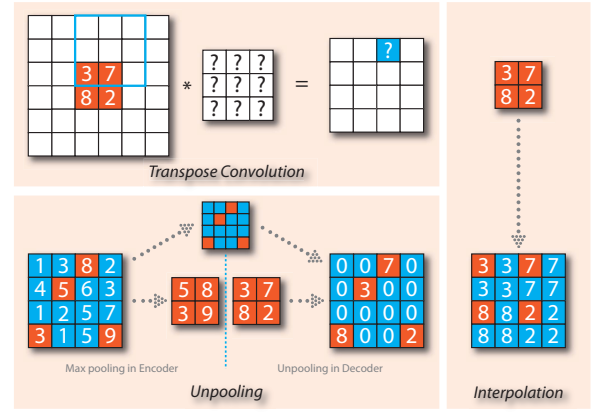


Figure 3: Upsampling methods. Transpose convolution is similar to convolution. It results in the checkerboard texture of the output. In interpolation, the inserted pixels are calculated by the existing pixels. Here we show the nearest neighbor interpolation. Unpooling simply uses zero to fill the inserted pixels, which also produces fake texture.

3.2 Upsampling

Upsampling is a technique that can improve the image resolution. There are three kinds of upsampling methods: unpooling, transpose convolution and interpolation. Figure 3 demonstrates the specific way of these methods. For GAN-based methods, the most commonly used interpolations are nearest neighbor interpolation, bilinear interpolation and bicubic interpolation. Here in Figure 3 we just show nearest neighbor interpolation as an example.

By analyzing the official implementation of **seven GAN-based face generation methods**, we find that only transpose convolution and interpolation have been used. IcGAN uses interpolation and others use transpose convolution.

Although only two methods are used, all of these three methods have been proved inducing fake texture. Google Brain [23] has proved that the transpose convolution results in the checkerboard texture of the output image. [36] has proved that the transpose convolution and nearest neighbor interpolation have fake texture. Though not mentioned explicitly, the process of their proof also points out that unpooling produces fake texture. For the remaining bilinear and bicubic interpolations, they bring periodicity into the second derivative signal of images [6]. This means that the interpolated images exist fake texture which can be detected by convolution kernel, for instance, Laplace operator.

4 PROPOSED METHOD

The fake texture produced by upsampling methods is totally different from the real texture in the real image. In this section, we firstly present the framework for face manipulation forensics by leveraging the imperfection of upsampling design in GANs.

Then, we propose the gray-scale fakeness prediction map to visualize the manipulated regions in fake images. The gray-scale fakeness prediction map is more informative than that of other localization methods. To ensure the effectiveness of gray-scale fakeness prediction map, we adopt a suitable loss function in Sec 4.3.

Finally, we introduce attention mechanism to generalize our approach in tackling unseen facial properties. The pipeline proposed

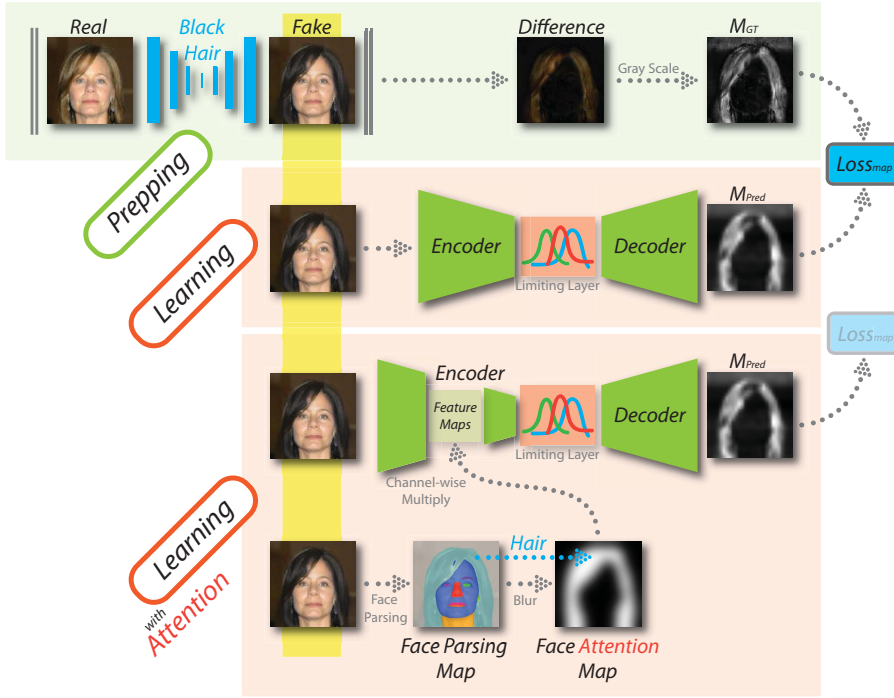


Figure 4: The framework of our proposed FakeLocator method. In the prepping procedure, we use pairs of real images and fake images to produce ground truth fakeness maps. In the learning procedure, the network is an encoder-decoder architecture. The inputs are real images or fake images while the outputs are gray-scale fakeness prediction maps. We use the gray-scale fakeness prediction maps and the ground truth fakeness maps corresponding to the inputs to calculate the loss. To improve the universality of the model, we introduce the attention mechanism into the model by using the face parsing module. We channel-wise multiply the face attention map with the feature maps of the encoder.

by us gives a full resolution prediction map. We also verify the robustness and universality of our method in Section 5.

Our method is designed for the imperfection of the upsampling methods and it is almost inevitable for GAN-based face generation methods to use upsampling methods. Thus our localization method is universal for all the GAN-based face generation methods. Furthermore, withing a better encoder-decoder network, our method will achieve better performance on fake localization problems.

4.1 Framework

Figure 4 shows the framework of our methodology. The backbone network is an encoder-decoder architecture. In our method, any encoder-decoder network can be used as the backbone network. The input is a fake image (X') while the output is a gray-scale fakeness prediction map (M_{Pred}).

$$M_{Pred} = \mathcal{G}_{dec}(\mathcal{G}_{enc}(X') \mapsto [0, 1]) \quad (1)$$

\mathcal{G}_{dec} and \mathcal{G}_{enc} are the decoder and encoder respectively. M_{GT} represents the ground truth fakeness map. In our method, the pixel values in the fakeness prediction map are real numbers. So we should fine-tune the network and limit the pixel values in the prediction fakeness prediction map. We add a limiting layer between the encoder and the decoder so that the pixel values could be limited to range within $[0,1]$. This limiting layer can also be added after the decoder. The loss (\mathcal{L}_{map}) is simply calculated by the following formula. Here \mathcal{L} will be introduced in subsection 4.3.

$$\mathcal{L}_{map} = \mathcal{L}(M_{Pred}, M_{GT}) \quad (2)$$

Furthermore, we add a classifier to the encoder-decoder architecture. It is just added for facilitating the calculation of the accuracy of detecting whether an image is real or fake. The classifier is not necessary for that we can judge the authenticity of the input image

through the fakeness prediction map. In the experiment, we have verified that the network with or without classifier has similar performance and they are both effective in locating fake regions.

In our further exploration, the universality of the model can be improved by adding a face parsing module. This module introduces the attention mechanism into the model. The details of the face parsing module will be introduced in section 4.4.

4.2 Gray-scale vs. Binary Fakeness Prediction Map

In the existing GAN-based face generation methods, even the best of them changes most of the pixels in the image when manipulating a property of the face. If we set the values of manipulated pixels as 1 while unmodified pixels as 0, then the fakeness prediction map does not catch the emphasis of the change in the figure.

To solve the problem, other localization methods [17, 28, 29] use the **binary fakeness prediction map**. They produce difference maps between real images and fake images and use a threshold to generate binary fakeness prediction maps from difference maps. The pixel values bigger than the threshold become 1 while the others become 0. However, the setting of a threshold is a big flop. Firstly, all the information about fake regions less than the threshold is omitted. Secondly, the threshold is usually a fixed value defined by experience, which does not work in all cases. Finally, the values of manipulated pixels in the fake image are all less than threshold if the fake image is slightly manipulated. The binary fakeness prediction map thus turns out to be entirely black and far from the truth.

Therefore, we discard the threshold when producing our fakeness prediction map. The training samples consist of two parts: input image and **gray-scale fakeness prediction map**. The input images fall into two categories, real images and fake images. For



Figure 5: From left to right: real image, fake image, gray-scale fakeness prediction map and binary fakeness prediction map

a training sample that regards the real image as the input image, the corresponding fakeness prediction map is a gray-scale map with all the pixel values equal to 0. This means in the current input image, there is no fake texture. On the other hand, if the input image is a fake image, the fakeness prediction map is obtained by the following calculating procedure.

As shown in Figure 5, these images in turn are real image (X), fake image (X'), gray-scale fakeness prediction map (M) and binary fakeness prediction map (B). $X, X' \in \mathbb{R}^{H \times W \times 3}$ and $M, B \in \mathbb{R}^{H \times W \times 1}$, where H, W are height and width of the these images. The fake image is produced by adding property p to the real image.

$$X' = \mathcal{G}_{dec, F}(\mathcal{G}_{enc, F}(X), p) \quad (3)$$

$\mathcal{G}_{dec, F}$ and $\mathcal{G}_{enc, F}$ are the decoder and encoder of the method F , $F \in \{\text{all the partial face manipulation GANs}\}$. To achieve the gray-scale fakeness prediction map, there are three steps as follows. 1) calculate the pixel difference between the real image and the fake image. 2) take the absolute value of the result and turn it into a gray-scale map. 3) divide each pixel by 255. Then each pixel value locates in the range of $[0, 1]$. Equation (4) shows the formula, in which $X_{i,j,k}, X'_{i,j,k}$ ($1 \leq i \leq H, 1 \leq j \leq W, 1 \leq k \leq 3, 0 \leq X_{i,j,k}, X'_{i,j,k} \leq 255$) are the value of a channel of a pixel of X and X' respectively. $M_{i,j}, B_{i,j}$ ($1 \leq i \leq H, 1 \leq j \leq W, 0 \leq M_{i,j} \leq 1, B_{i,j} \in \{0, 1\}$) are the value of a pixel of M and B respectively. *Gray* is a function converts an RGB pixel to a gray-scale pixel.

$$M_{i,j} = \text{Gray}(|X_{i,j,k} - X'_{i,j,k}|)/255 \quad (4)$$

For the full face synthesis, the fakeness prediction map is a gray-scale map with all the pixel values equal to 1. The gray-scale fakeness prediction map clearly depicts the difference between real and fake images and highlights the regions with large differences.

4.3 Loss Function

For the gray-scale fakeness prediction map, we have tried four loss functions. Two of them are L1 loss and L2 loss, which commonly used in regression problems. The other two are Focal loss [18] and Dice loss [30], which commonly used in traditional segmentation problems. In the experiment, we find that L1 loss and L2 loss are better choices than the others. This means for gray-scale fakeness prediction maps, regression losses are better than traditional segmentation losses. The comparison is shown in Table 2. The formulas of L1 and L2 are shown in Equation (5,6). $X_{i,j}$ and $Y_{i,j}$ ($1 \leq i \leq H, 1 \leq j \leq W$) represent the pixel in the prediction gray-scale fakeness prediction map and ground truth of the gray-scale fakeness prediction map respectively, where H, W are the



Figure 6: From left to right: input image (hair property modified), face parsing map, region map of the modified property, face attention map

height and width of the maps.

$$\mathcal{L}_{1\text{loss}} = \frac{1}{n} \sum |X_{i,j} - Y_{i,j}| \quad (5)$$

$$\mathcal{L}_{2\text{loss}} = \frac{1}{n} \sum |X_{i,j} - Y_{i,j}|^2 \quad (6)$$

The formula of Focal loss is shown below in Equation (7,8). Assume $p \in [0, 1]$ is the model's estimated probability for the class with label $y = 1$.

$$p_t = \begin{cases} p & y = 1 \\ 1 - p & \text{otherwise} \end{cases} \quad (7)$$

$$FL(p_t) = -\alpha_t (1 - p_t)^\gamma \log(p_t) \quad (8)$$

α_t is similar defined as p_t . The focusing parameter γ smoothly adjusts the rate at which easy examples are down-weighted.

The formula of Dice loss is shown below in Equation (9). A and B represent the point set of ground truth and prediction respectively.

$$\mathcal{L}_{\text{Dice}} = \frac{2|A \cap B|}{|A| + |B|} \quad (9)$$

4.4 Face Parsing

Although the GAN-based face generation methods can change facial properties very well, they still inevitably modify the pixels in other regions of the image. Therefore, they use some methods (e.g., skip connection) to repair the fake images by referring to the real ones, which makes the region out of modified properties not totally fake. Only the regions of modified properties are full of fake textures. To learn the fake textures better, we introduce attention mechanism into our method by using face parsing module.

As shown in Figure 4, we use face parsing to mark the area corresponding to the modified property and insert the face attention map into the encoder. The attention mechanism urges the model to put more emphasis on the regions of modified property, which improves the universality of the model. In the learning procedure, the face attention map is calculated by the face parsing module. In the testing procedure, the face attention map is a white map which does not provide any region information and reserve the original information of feature maps in the encoder.

As shown in Figure 6, we demonstrate the face attention map corresponding to the modified property *Hair*. The images in turns are the input image which modifies *Black Hair* property, face parsing map, region map of the modified property, face attention map. To produce the face attention map, there are three steps. First, use a face parsing method to generate face parsing map with the input image. Second, choose the region of the modified property. Third, use the blur method to expand the light region. The reason why

we add the third step is that the region out of modified properties also has the reference significance. However, the weight of them should not be higher than the regions of modified properties. The blur method is suitable for this transformation.

5 EXPERIMENTAL RESULT

5.1 Experimental Setup

Databases: Our experiment benchmarks the real face databases CelebFaces Attributes (CelebA) [20] and Flickr-Faces-HQ (FFHQ) [13]. CelebA contains 202,599 face images of celebrities, each annotated with 40 binary attributes. FFHQ contains 70,000 high-quality images. The database includes vastly more variation than CelebA in terms of age, ethnicity and image background.

The real images are from CelebA and FFHQ databases. The fake images are produced by seven GAN-based face generation methods and their corresponding databases and properties, as shown in Table 1. The images are all in PNG format. We use **Entire** to represent the property of the images produced by full face synthesis methods.

Table 1: Properties of GANs. We choose the facial properties which well modified by these GANs.

STGAN (CelebA)	AttGAN (CelebA)
Bald, Bangs, Black hair, Blond hair, Smile, Brown hair, Eyeglasses, Male, Mustache	Bald, Bangs, Black hair, Blond hair, Brown hair, Eyeglasses, Male, Smile
StarGAN (CelebA)	IcGAN (CelebA)
Black hair, Blond hair, Brown hair, Gender, Age	Bald, Bangs, Eyeglasses, Smile
StyleGAN (FFHQ)	PGGAN (FFHQ), StyleGAN (FFHQ), StyleGAN2 (FFHQ)
Smile, Age, Gender	Entire

Settings: The experiment runs on a Ubuntu 16.04 system with an Intel(R) Xeon(R) CPU E5-2699 with 196 GB of RAM. The server also has a NVIDIA RTX 2080ti GPU with 11GB of RAM. In the experiment, we train for 10 iterations with an ADAM [15] optimizer whose $\alpha = 0.0001$, $\beta_1 = 0.99$, $\beta_2 = 0.999$, and weight decay = 10^{-7} . The minibatch size of every training and validation dataset is 8.

Training and Testing Dataset: In the seven GAN-based face generation methods, STGAN is the newest GAN-based method in partial face manipulation and achieves state-of-the-art results. Thus we choose it as the main experiment object to demonstrate our method. Of course, we also confirm the availability of our method on other GANs, which is also shown in Figure 1 and Table 3.

For each facial property, we train the model with 5,000 persons' real images and fake images of other different 5,000 persons. In the test dataset, we use 1,000 real images and 1,000 fake images for performance evaluation of the classification metric. For the metrics of localization, we reuse the 1,000 fake images. The images in the test and training dataset are totally different identities.

Network: Any encoder-decoder network is feasible in our framework. In the accessible networks, we choose the Deeplabv3 architecture as our backbone network. Deeplabv3 has a good performance in segmentation and Pytorch [24] provides a pre-trained Deeplabv3-ResNet101 model. Deeplabv3-ResNet101 is constructed by a Deeplabv3 model with a ResNet-101 backbone. The pre-trained model has been trained on a subset of COCO train2017, on the 20 categories that are present in the Pascal VOC dataset. We fine-tune

Table 2: Loss Function Comparison

	ACC	COSS	PSNR	SSIM
Baseline [Stehouwer'19]	1.0	0.5008	5.17	0.1591
L1 Loss (no cl)	\	0.9271	22.54	0.7533
L1 Loss	0.994	0.8887	22.83	0.7823
L2 Loss	1.0	0.9228	23.09	0.7497
Dice Loss	0.990	0.7633	12.89	0.3585
Focal Loss	0.984	0.3988	20.79	0.3301

the network and use **Sigmoid** function as the limiting layer. The input size supported by Deeplabv3-ResNet101 is 224x224, thus we resized all the input images to this size. Other encoder-decoder networks are also available.

Metrics: We report accuracy (ACC) for classification and use cosine similarity (COSS), peak signal-to-noise ratio (PSNR) and structural similarity (SSIM) for fakeness prediction map. COSS is a measure of similarity between two non-zero vectors of an inner product space that measures the cosine of the angle between them. We transform the image into a vector before calculating COSS. PSNR is the most commonly used measurement for the reconstruction quality of lossy compression. SSIM is used for measuring the similarity between two images. ACC, COSS, PSNR and SSIM metrics are better if a higher value is provided. The value ranges of ACC, COSS and SSIM are all in [0,1].

5.2 Results and Analysis

To evaluate the effectiveness, robustness and universality of our method, experiments try to answer the following five research questions:

RQ1: What is the performance of our method and which loss function is more suitable for gray-scale fakeness prediction map? In Table 2, we show a comparison of our method and the **Baseline**. The table also shows the comparison of results with different loss function strategies. Here we choose *Bald* of STGAN as the property of fake images. In the first column, **Baseline** represents the result of [29]. We enlarge its binary fakeness prediction maps to the size of 224x224 before calculating the metrics. The label *no cl* means the model does not have a classifier.

As mentioned in section 1, **FaceForensics++** only contains face identity and expression swap, which is not enough for showing the effect of fake localization methods. Therefore, we build a dataset generated by GAN-based face generation methods that manipulate facial properties by ourselves. Only [29] working on the same topic as us. So we choose their method as the **Baseline**. Because we have explained the shortcoming of **Baseline** method theoretically, so we just use one property *Bald* to show the higher performance of our method. It is obvious that, compared to **Baseline**, the gray-scale fakeness prediction maps predicted by our method not only have a higher resolution, but also a better performance (several times higher). Moreover, the performance is distinctly higher on all the other properties and GAN-based face generation methods.

Moreover, using the same loss function, Deeplabv3 with/without classifier achieves a similar value on metrics. Thus the classifier used to calculate ACC does not affect the fakeness prediction map. The highest value of PSNR and SSIM are achieved by L1 loss and L2 loss respectively. Their performances are approximate and better than other loss functions. We can conclude that the loss functions

Table 3: Performance of The Model

	STGAN						StyleGAN				StarGAN			AttGAN			IcGAN	PGGAN	StyleGAN2
	Smile	Bangs	Bald	Mustache	Eyeglasses	Black hair	Age	Gender	Smile	Entire	Age	Gender	Black hair	Bald	Smile	Eyeglasses	Bald	Entire	Entire
ACC	0.9985	0.9985	0.9985	0.9935	0.997	0.9985	0.9985	0.999	0.999	0.921	0.999	0.999	0.999	0.9985	0.9985	0.9985	0.9995	0.9775	0.855
PSNR	34.72	33.07	27.51	36.59	33.23	31.05	20.71	18.92	22.68	55.08	26.38	26.71	25.25	25.31	29.49	28.19	17.57	48.70	72.00
SSIM	0.9086	0.9033	0.8572	0.8829	0.8663	0.9029	0.6159	0.5726	0.6625	0.8268	0.7929	0.7952	0.7911	0.7839	0.8736	0.8207	0.6002	0.8945	0.9262
COSS	0.8634	0.8850	0.9014	0.9152	0.9093	0.8817	0.7479	0.7580	0.7365	0.9174	0.8494	0.8416	0.8780	0.8883	0.8277	0.8313	0.8352	0.9972	0.9678

Table 4: Universal Test

	STGAN	AttGAN			STGAN	StyleGAN		
	Bald	Bald	Black hair	Eyeglasses	Smile	Smile	Age	Gender
ACC	0.994	0.973	0.513	0.519	1.0	0.588	0.593	0.588
PSNR	22.83	21.46	22.84	23.52	35.49	20.85	18.59	16.50
SSIM	0.7823	0.6688	0.3966	0.4168	0.9218	0.5571	0.4958	0.4301
COSS	0.8887	0.8141	0.6932	0.6950	0.8844	0.6176	0.3141	0.6470

Table 5: Comparison of the model with and without face parsing

	Black hair		Brown hair		Smile	
	no FP	with FP	no FP	with FP	no FP	with FP
ACC	0.237	0.67	0.588	0.859	0.448	0.752
PSNR	28.270	25.296	30.611	21.926	41.836	40.723
SSIM	0.783	0.825	0.854	0.802	0.989	0.990
COSS	0.855	0.817	0.876	0.863	0.803	0.808

outstanding in regression problems are better for gray-scale fake-ness prediction map. In the following experiments, considering the sake of unity, we choose L1 loss as the default loss function.

RQ2: Whether our approach is generic to different GANs and facial properties with the same GANs? In the experiment, we find that our method is efficient for all the GANs and their specified facial properties. Hence there is a further question. Is the model trained on one GAN is effective for other GANs?

As shown in Table 4, we demonstrate some of the test results. Here are two different test pairs. The model trained from STGAN (Bald) tests properties of AttGAN and the model trained from STGAN (Smile) tests properties of StyleGAN. The gray columns are the first column of each test pair. It records the value of the model testing on the test dataset of itself, which is used as the reference substance. For each test pair, the three columns right beside the gray column are the performance of the model on other datasets.

We can find that the model trained by one GAN and specified property is more effective on other GANs with the same dataset and property than the GANs with different datasets or properties. Furthermore, in our observation from massive experiments, the model trained by one GAN and specified property also does not have a good performance on the same GAN with other properties. To solve this problem, we introduce the method in the next question.

RQ3: How to improve the universality of the method?

We train a model with many single-face-property fake images. We select STGAN, StyleGAN, AttGAN, StarGAN, IcGAN, PGGAN, StyleGAN2 and all their properties. Each category $C_{i,j}$ ($i \in \text{GANs}$, $j \in \text{Properties of GANs(i)}$) supports 2,000 fake images into the training dataset. There are totally of 64,000 fake images and 64,000 real images randomly selected in CelebA and FFHQ. The model performs well on the test dataset, which is shown in Table 3. The gray-scale fakeness prediction maps corresponding to these metric values are referred to Figure 1. In addition, even though the model uses a lot of GANs and properties for training, in the testing dataset, it only labels the location of fake regions of the modified facial properties. This is a nice phenomenon which demonstrates that the model has learned to recognize the fake textures and distinguish them. This method not only improves the universality, but also improves the performance. The metric value of STGAN (Bald) is significantly higher than that in Table 2.

RQ4: How to improve the universality of the method on unseen facial properties? If the facial properties are known by

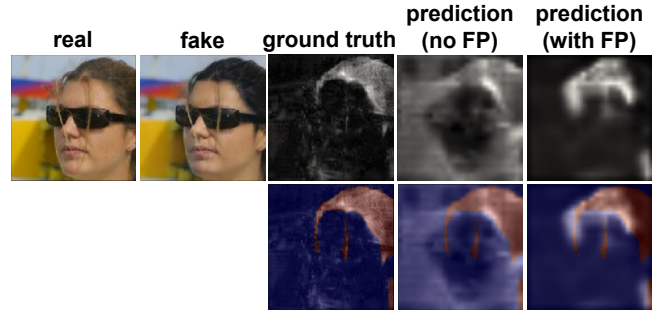


Figure 7: Result of the models (with face parsing and model without face parsing) testing on STGAN (Black hair). The models are trained on STGAN (Blond hair). The first row in turn shows the real image, fake image, ground truth, prediction without face parsing, prediction with face parsing. The second row shows the regions where we used to calculate similarity metrics.

us, the method mentioned above is useful. However, sometimes the fake images are modified with unseen facial properties. Here we introduce a method which improves the universality of the model on unseen facial properties.

As introduced in Figure 4, through adding face attention information, the model can learn fake texture better. In the testing procedure, we use a white map that does not provide any location information as the face attention map. The result shows that the model does learn fake texture better. As an example, we train two models on STGAN (Blond hair). One has face attention information while the other does not. In Figure 7, we demonstrate the localization performance of the model testing on STGAN (Black hair). **FP** means face parsing. The model with face parsing achieves a better result. It can capture main fake textures while the model without face parsing is in a mess.

Because this is a cross-property test, so we use in-region similarity to compare the results with ground truth. In-region means the region of the modified property. In Figure 7, it represents the red region of the image in the second row.

In Table 5, we show the testing performance on STGAN (Black hair), STGAN (Brown hair) and STGAN (Smile) of the model trained by STGAN (Blond hair). The similarity metrics between the model with face parsing or model without face parsing are approximate. However, the detection accuracy of the model with face parsing is much better than that without face parsing. In Figure 7, we can also

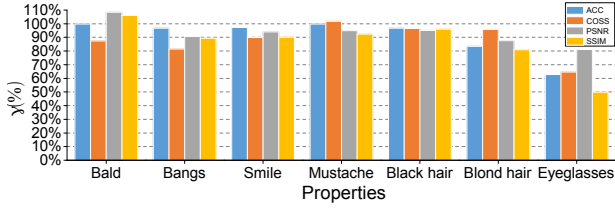


Figure 8: Comparison with no disorganization. γ means the percentage of the metric values compared with no disorganization.



Figure 9: Disorganization test result. This is the property *Blond hair* of STGAN. We clip the image into four pieces and mess up their order. This operation is for verifying whether our model is location independent. The result shows that our model is robust to this test.

find that model with parsing can catch fake regions more accurately. To the model without face parsing, if we change facial property *Hair* with different colors, the universality of it will reduce. To the model with face parsing, it learns fake texture better with the introduction of attention mechanism, which leads to a better universality. It even gets a good detection accuracy on facial property *Smile*, which is very different from facial property *Hair*.

RQ5: How robust is the model in tackling different deformations? It is very necessary to test the robustness of the localization model. In the real world, images may be degraded by various operations such as compression, low-resolution, etc. Moreover, we also need to ensure that the model can locate fake texture in any place. This means the model is location independent.

To test the robustness of our model, we use two different test directions. First, we crop each fake image uniformly into four pieces and splice them randomly, which is called *disorganization test*. The purpose of this test is to verify whether the model is strongly correlated to the location, namely it just remembers the location instead of recognizing the fake texture. Figure 8 shows the percentage of the metric values compared to that before disorganization test. The model performance is just a little worse than the formal situation. Figure 9 shows the prediction result of the disorganization test.

We also apply four different real-world facial image degradations (**JPEG Compression**, **Blur**, **Noise**, and **Low-resolution**) on 1,000 fake images. The gray-scale fakeness prediction map is processed by the real image and the degraded fake image. In Figure 10, the vertical axis of all the four subfigures represents the percentage of the metric values compared to that before degradation. **JPEG Compression** means converting an image from PNG format to JPEG format. The horizontal axis of the image represents the compression quality during conversion. **Blur** and **Noise** mean applying Gaussian blur and Gaussian noise to fake images respectively. The horizontal axis respectively represents the filter size of the Gaussian blur and the variance of the Gaussian noise. **Low-resolution** means resizing the fake image to a low resolution, then restoring

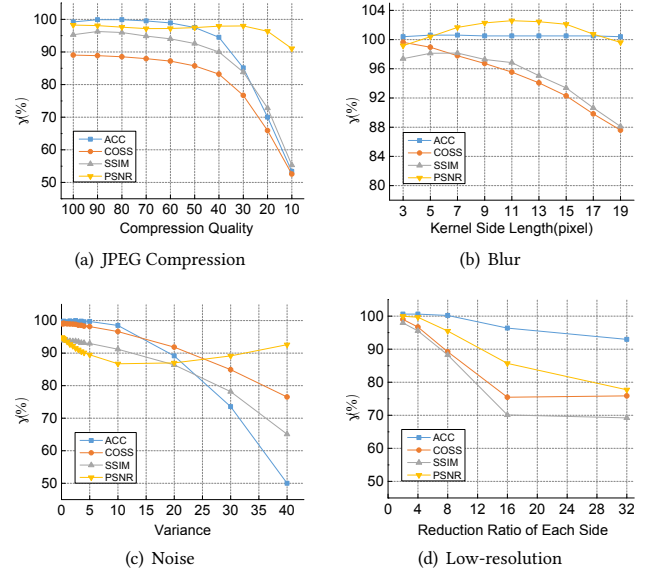


Figure 10: Anti-degradation capability Of the model. γ means the percentage of the metric values compared with no degradation.

to the original resolution. The quality of the fake image reduces in resizing procedure. The horizontal axis represents the reduction ratio of each side of the image.

We can find that all the metric values gradually reduce in **Low-resolution**. In the other three degradations, **PSNR** achieves only minor changes, while **ACC**, **COSS** and **SSIM** decrease when the interference is extremely high. Overall, our methodology performs well against various degradations.

6 CONCLUSION

In this paper, we utilize the imperfection of the upsampling procedure in all the GAN-based partial face manipulation methods and full face synthesis methods. This imperfection can be used for fake detection and fake localization. Thus we propose a universal pipeline to solve the fake localization problem. Through using a gray-scale fakeness prediction map, we achieve the SOTA localization accuracy. As an improvement of the universality of the model, the attention mechanism is inserted into the encoder-decoder architecture by using face parsing information. The model is robustness to real-world degradations such as blur, compression, etc.

Beyond DeepFake detection and localization, we conjecture that the FakeLocator is capable of detecting and localizing non-additive noise adversarial attacks such as [1, 8, 9, 34] where the attacked images do not exhibit visual noise pattern and are usually much harder to detect accurately. Moreover, the combined effort of the proposed method in tandem with fake voice detector [32] or detector in other modality [26] can and will potentially provide more comprehensive defense mechanism against video-based DeepFakes along with their enhanced variant [11].

In future work, we think there are two ways deserve research. One is to propose better localization methods which are useful to unseen GAN methods through exploiting the imperfection of

upsampling methods. The other is to visualize the fake texture in each image and classify them according to different GANs and upsampling methods.

REFERENCES

- [1] Yupeng Cheng, Qing Guo, Felix Juefei-Xu, Xiaofei Xie, Shang-Wei Lin, Weisi Lin, Wei Feng, and Yang Liu. 2020. Pasadena: Perceptually Aware and Stealthy Adversarial Denoise Attack. *arXiv preprint* (2020).
- [2] Yunjei Choi, Minje Choi, Munyoung Kim, Jung-Woo Ha, Sunghun Kim, and Jaegul Choo. 2018. Stargan: Unified generative adversarial networks for multi-domain image-to-image translation. In *Proceedings of the IEEE Conference on Computer Vision and Pattern Recognition*. 8789–8797.
- [3] François Chollet. 2017. Xception: Deep learning with depthwise separable convolutions. In *Proceedings of the IEEE conference on computer vision and pattern recognition*. 1251–1258.
- [4] L. Dang, Syed Hassan, Suhyeon Im, Jaechol Lee, Sujin Lee, and Hyeonjoon Moon. 2018. Deep learning based computer generated face identification using convolutional neural network. *Applied Sciences* 8, 12 (2018), 2610.
- [5] deepfakes. 2017. faceswap. <https://github.com/deepfakes/faceswap>.
- [6] Andrew C Gallagher. 2005. Detection of Linear and Cubic Interpolation in JPEG Compressed Images.. In *CRV*, Vol. 5. Citeseer, 65–72.
- [7] Ian Goodfellow, Jean Pouget-Abadie, Mehdi Mirza, Bing Xu, David Warde-Farley, Sherjil Ozair, Aaron Courville, and Yoshua Bengio. 2014. Generative adversarial nets. In *Advances in neural information processing systems*. 2672–2680.
- [8] Qing Guo, Felix Juefei-Xu, Xiaofei Xie, Lei Ma, Jian Wang, Bing Yu, Wei Feng, and Yang Liu. 2020. Watch out! Motion is Blurring the Vision of Your Deep Neural Networks. *arXiv preprint arXiv:2002.03500* (2020).
- [9] Qing Guo, Xiaofei Xie, Felix Juefei-Xu, Lei Ma, Zhongguo Li, Wanli Xue, Wei Feng, and Yang Liu. 2020. SPARK: Spatial-aware Online Incremental Attack Against Visual Tracking. *arXiv preprint arXiv:1910.08681* (2020).
- [10] Zhenliang He, Wangmeng Zuo, Meina Kan, Shiguang Shan, and Xilin Chen. 2019. Attgan: Facial attribute editing by only changing what you want. *IEEE Transactions on Image Processing* (2019).
- [11] Yihao Huang, Felix Juefei-Xu, Run Wang, Qing Guo, Lei Ma, Xiaofei Xie, Jianwen Li, Weikai Miao, Yang Liu, and Geguang Pu. 2020. FakePolisher: Making DeepFakes More Detection-Evasive by Shallow Reconstruction. *arXiv preprint* (2020).
- [12] Tero Karras, Timo Aila, Samuli Laine, and Jaakko Lehtinen. 2017. Progressive growing of gans for improved quality, stability, and variation. *arXiv preprint arXiv:1710.10196* (2017).
- [13] Tero Karras, Samuli Laine, and Timo Aila. 2019. A style-based generator architecture for generative adversarial networks. In *Proceedings of the IEEE Conference on Computer Vision and Pattern Recognition*. 4401–4410.
- [14] Tero Karras, Samuli Laine, Miika Aittala, Janne Hellsten, Jaakko Lehtinen, and Timo Aila. 2019. Analyzing and Improving the Image Quality of StyleGAN. *arXiv preprint arXiv:1912.04958* (2019).
- [15] Diederik P Kingma and Jimmy Ba. 2014. Adam: A method for stochastic optimization. *arXiv preprint arXiv:1412.6980* (2014).
- [16] Dave Lee. 2018. Deepfakes porn has serious consequences. <https://www.bbc.com/news/technology-42912529>.
- [17] Lingzhi Li, Jianmin Bao, Ting Zhang, Hao Yang, Dong Chen, Fang Wen, and Baining Guo. 2019. Face X-ray for More General Face Forgery Detection. *arXiv preprint arXiv:1912.13458* (2019).
- [18] Tsung-Yi Lin, Priya Goyal, Ross Girshick, Kaiming He, and Piotr Dollár. 2017. Focal loss for dense object detection. In *Proceedings of the IEEE international conference on computer vision*. 2980–2988.
- [19] Ming Liu, Yukang Ding, Min Xia, Xiao Liu, Errui Ding, Wangmeng Zuo, and Shilei Wen. 2019. STGAN: A Unified Selective Transfer Network for Arbitrary Image Attribute Editing. In *Proceedings of the IEEE Conference on Computer Vision and Pattern Recognition*. 3673–3682.
- [20] Ziwei Liu, Ping Luo, Xiaogang Wang, and Xiaoou Tang. 2018. Large-scale celebfaces attributes (celeba) dataset. *Retrieved August 15* (2018), 2018.
- [21] Huaxiao Mo, Bolin Chen, and Weiqi Luo. 2018. Fake faces identification via convolutional neural network. In *Proceedings of the 6th ACM Workshop on Information Hiding and Multimedia Security*. ACM, 43–47.
- [22] Huy H Nguyen, Fuming Fang, Junichi Yamagishi, and Isao Echizen. 2019. Multi-task Learning For Detecting and Segmenting Manipulated Facial Images and Videos. *arXiv preprint arXiv:1906.06876* (2019).
- [23] Augustus Odena, Vincent Dumoulin, and Chris Olah. 2016. Deconvolution and Checkerboard Artifacts. *Distill* (2016). <https://doi.org/10.23915/distill.00003>
- [24] Adam Paszke, Sam Gross, Francisco Massa, Adam Lerer, et al. 2019. PyTorch: An imperative style, high-performance deep learning library. In *Advances in Neural Information Processing Systems*. 8024–8035.
- [25] Guim Perarnau, Joost van de Weijer, Bogdan Raducanu, and Jose M. Álvarez. 2016. Invertible Conditional GANs for image editing. In *NIPS Workshop on Adversarial Training*.
- [26] Hua Qi, Qing Guo, Felix Juefei-Xu, Xiaofei Xie, Lei Ma, Wei Feng, Yang Liu, and Jianjun Zhao. 2020. DeepRhythm: Exposing DeepFakes with Attentional Visual Heartbeat Rhythms. *arXiv preprint* (2020).
- [27] Andreas Rössler, Davide Cozzolino, Luisa Verdoliva, Christian Riess, et al. 2019. Faceforensics++: Learning to detect manipulated facial images. *arXiv preprint arXiv:1901.08971* (2019).
- [28] Kritaphat Songsri-in and Stefanos Zafeiriou. 2019. Complement Face Forensic Detection and Localization with Facial Landmarks. *arXiv preprint arXiv:1910.05455* (2019).
- [29] Joel Stehouwer, Hao Dang, Feng Liu, Xiaoming Liu, and Anil Jain. 2019. On the Detection of Digital Face Manipulation. *arXiv preprint arXiv:1910.01717* (2019).
- [30] Carole H Sudre, Wenqi Li, Tom Vercauteren, Sebastien Ourselin, and M Jorge Cardoso. 2017. Generalised dice overlap as a deep learning loss function for highly unbalanced segmentations. In *Deep learning in medical image analysis and multimodal learning for clinical decision support*. Springer, 240–248.
- [31] Daniel Thomas. 2020. Deepfakes: A threat to democracy or just a bit of fun? <https://www.bbc.com/news/business-51204954>.
- [32] Run Wang, Felix Juefei-Xu, Yihao Huang, Qing Guo, Xiaofei Xie, Lei Ma, and Yang Liu. 2020. DeepSonar: Towards Effective and Robust Detection of AI-Synthesized Fake Voices. *arXiv preprint arXiv:2005.13770* (2020).
- [33] Run Wang, Felix Juefei-Xu, Lei Ma, Xiaofei Xie, Yihao Huang, Jian Wang, and Yang Liu. 2019. FakeSpotter: A Simple yet Robust Baseline for Spotting AI-Synthesized Fake Faces. *arXiv:1909.06122 [cs.CR]*
- [34] Run Wang, Felix Juefei-Xu, Xiaofei Xie, Lei Ma, Yihao Huang, and Yang Liu. 2019. Amora: Black-box Adversarial Morphing Attack. *arXiv preprint arXiv:1912.03829* (2019).
- [35] Ning Yu, Larry S Davis, and Mario Fritz. 2019. Attributing fake images to gans: Learning and analyzing gan fingerprints. In *Proceedings of the IEEE International Conference on Computer Vision*. 7556–7566.
- [36] Xu Zhang, Svebor Karaman, and Shih-Fu Chang. 2019. Detecting and Simulating Artifacts in GAN Fake Images. *arXiv preprint arXiv:1907.06515* (2019).